Published in final edited form as:
Neuroimage. 2010 July 1; 51(3): 1089–1097. doi:10.1016/j.neuroimage.2010.03.045.

In vivo Quantitative evaluation of brain tissue damage in Multiple Sclerosis using Gradient Echo Plural Contrast Imaging technique

Pascal Sati[1], **Anne H. Cross**[2], **Jie Luo**[3], **Charles F. Hildebolt**[1], and **Dmitriy A. Yablonskiy**[1,4]

[1]Department of Radiology, Washington University in St Louis, One Brookings Drive, Saint Louis, MO 63130, USA

[2]Department of Neurology, Washington University in St Louis, One Brookings Drive, Saint Louis, MO 63130, USA

[3]Department of Chemistry, Washington University in St Louis, One Brookings Drive, Saint Louis, MO 63130, USA

[4]Department of Physics, Washington University in St Louis, One Brookings Drive, Saint Louis, MO 63130, USA

Abstract

Conventional MRI based on weighted spin-echo (SE) images aids in the diagnosis of multiple sclerosis (MS); however, MRI markers derived from SE sequences provide limited information about lesion severity and correlate poorly with patient disability assessed with clinical tests. In this study, we introduced a novel method [based on quantitative R2* (1/T2*) histograms] for estimating the severity of brain tissue damage in MS lesions. We applied at 1.5 T an advanced, multi-gradient-echo MRI technique [gradient echo plural contrast imaging (GEPCI)] to obtain images of the brains of healthy control subjects and subjects with MS. GEPCI is a simple yet robust technique allowing simultaneous acquisition of inherently co-registered quantitative T2* and FLAIR-like maps, along with T1-weighted images within a clinically acceptable time frame. Images obtained with GEPCI appear highly similar to standard scans; hence, they can be used in a reliable and conventional way for a clinical evaluation of the disease. Yet, the main advantage of GEPCI approach is its quantitative nature. Analysis of R2* histograms of white matter revealed a difference in the distribution between healthy subjects and subjects with MS. Based on this difference, we developed a new method for grading the severity of tissue damage [tissue-damage score (TDS)] in MS lesions. This method also provides a tissue damage load (TDL) assessing both lesion load and lesion severity, and a mean tissue damage score (MTDS) estimating the average MS lesion damage. We found promising correlations between the results derived from this method and the standard measure of clinical disability.

Introduction

Multiple sclerosis is a common disease, affecting 2.5 million people world-wide. The clinical course is heterogeneous, ranging from benign disease in which patients live an almost normal life to severe and devastating disease that may shorten life. Demyelination, axonal loss, remyelination, and inflammation are key components of MS pathology in the human central

Manuscript correspondence: Dmitriy A. Yablonskiy, PhD, Mail: East Imaging Building, Biomedical MR Laboratory, 4525 Scott Ave, Saint Louis, MO 63110, USA., Telephone: 314-362-1815, Fax: 314-362-0526, YablonskiyD@wustl.edu.

nervous system (CNS) (Lucchinetti et al. 2000; Bjartmar et al. 2003). As a non-invasive tool, magnetic resonance imaging (MRI) plays a large role in clinical diagnosis and evaluation of patients with MS (Simon 2005; Chitnis and Pirko 2009). Conventional spin-echo (SE) sequences such as T1-weighted SE (T1W-SE), T2-weighted SE (T2W-SE) and fluid-attenuated inversion recovery (FLAIR) imaging techniques are useful in the clinical setting (Sicotte et al. 2003; Traboulsee and Li 2008). While these conventional sequences aid in MS diagnosis, thus far they have provided limited information about the severity of the underlying pathology. Currently, T1W-SE sequence is the only conventional sequence that provides information about the severity of the MS lesion. It does this by detecting so-called “black holes” (Barkhof et al. 1998; van Walderveen et al. 1998) which have more severe underlying tissue damage than MS lesions seen only with T2W-SE sequences. In addition, the standard MR volumetric markers (such as lesion load) obtained from these sequences correlate poorly with MS disability assessed by clinical tests, the so-called “MRI paradox” (Fulton et al. 1999; Mainero et al. 2001). This paradox has been attributed to the complexity and heterogeneity of the underlying tissue damage in MS, to the different effects on function caused by different lesion locations, as well as to variable degrees of neural plasticity among patients. The paradox might also be due to the lack of quantitative information about the severity of the lesions (level of tissue damage). Indeed, the information about the black holes provided by T1W-SE sequence remains qualitative and is also limited in that black holes constitute only a small portion of the typical MS lesion load. Moreover, the image contrast in the standard “weighted” spin-echo sequence depends not only on the MR relaxation time constants of the brain tissue but also on the parameters of the pulse sequence. This non-biological dependence may lead to an incorrect estimation of the black hole load as lesions may not be apparent when image contrast is poor. These shortcomings can be overcome by using recently-proposed approaches based on measuring T2 and T1 relaxation times instead of using T2- and T1-weighted images. Q*uantitative* maps of T2 and T1 brain tissue relaxation times were used to demonstrate global differences between normal subjects and subjects with MS (Barbosa et al. 1994; Barkhof and van Walderveen 1999; Stevenson et al. 2000; Grenier et al. 2002; Parry et al. 2002; Vaithianathar et al. 2002; Vrenken et al. 2006; Neema et al. 2009). In more recent studies, different types of MS abnormalities were delineated with T2 mapping (Papanikolaou et al. 2004), and strong correlations between relaxation times and MS-pathology severity were reported (Schmierer et al. 2008; Seewann et al. 2009). This is an important result demonstrating that physical mechanisms responsible for MR relaxation processes are sensitive to the tissue microstructure and tissue composition. None of these differences has, however been used for *in vivo* assessment of MS lesion severity. One obstacle is that obtaining high resolution quantitative T2 or T1 maps can require long acquisition times (4.5 hours in (Papanikolaou et al. 2004)).

There is, however, another tissue-specific relaxation-time constant (T2*) that has not yet been fully exploited for patients with MS. Our group recently introduced a MRI-based, gradient echo plural contrast imaging (GEPCI) technique (Yablonskiy 2000a; Yablonskiy 2000b; Yablonskiy 2003; Bashir and Yablonskiy 2006) that generates quantitative T2* maps, quantitative FLAIR-like images and T1-weighted images from a single scan. Using the GEPCI technique to measure T2* offers many advantages (rapid acquisition, multi-contrast images, inherent co-registration, and low RF-power deposition that is especially important for high-field MRI) over other relaxometry techniques. Moreover, this technique is appropriate for standard evaluation of patients with MS as demonstrated by our preliminary results (Bashir et al. 2007; Sati et al. 2008a; Sati et al. 2008b; Sati et al. 2009a; Sati et al. 2009b; Sati et al. 2009c).

In this pilot study, we illustrate advantages of the GEPCI technique for evaluation of MS lesions. Based on tissue R2* maps, we also introduce a new scoring method that allows quantitative evaluation of the severity of brain-tissue damage in MS lesions.

Materials and methods

Subjects and Study Design

The study was approved by the Institutional Review Board of Washington University School of Medicine and informed written consent was obtained from all the subjects. Five subjects with clinically definite MS (Lublin and Reingold 1996) entered the study. Subjects with MS had the following characteristics: 3 females, 2 males; mean age = 43.2 years [standard deviation (SD) = 9.5 years]; 4 with relapsing remitting (RRMS) disease and one with secondary progressive (SPMS) disease. All subjects underwent a 1.5T brain MR imaging examination followed by a clinical examination on the same day. Physical disability was rated using the expanded disability status scale (EDSS) (Kurtzke 1983). Five healthy controls were also recruited for a 1.5T brain MR imaging examination only. Healthy subjects had the following characteristics: 3 females, 2 males, with mean age = 35.8 years (SD =15.8 years).

Image Acquisition

MRI was performed with a 1.5T whole-body MR scanner (Magnetom Sonata, Siemens Medical Solutions, Erlangen, Germany), available for research in the East Building Imaging Center (Department of Radiology, Washington University). For signal reception, a CP head coil was used. Forty-four contiguous 3-mm axial imaging sections were obtained with a 24-cm field-of-view (FOV), a matrix size of 256 × 192, and using two types of Turbo SE (TSE) sequences: 1) T2-weighted images with TR = 6800 ms and TE = 95 ms, Bandwidth=151 Hz/Px, Turbo factor=7; 2) FLAIR images with TI = 2310 ms, TR = 10000 ms and TE = 83 ms, Bandwidth=219 Hz/Px, Turbo factor=13; plus a standard SE sequence: T1-weighted images with TR = 600 ms and TE = 12 ms, Bandwidth=130 Hz/Px; Total time for these three standard sequences was 16 minutes.

Three dimensional (3D) version of the GEPCI pulse sequence (Figure 1) (Yablonskiy 2000a) was acquired using forty axial partitions (slices) with a 256 × 256 matrix (voxel resolution of $1 \times 1 \times 3\ mm^3$). For each slice, thirteen gradient-echo images were generated with TR = 50 ms, first gradient echo time TE1 = 3.4 ms, gradient echo spacing of 3.4 ms, and flip angle of 30°. Acquisition time for the GEPCI sequence was 8 min 32 s.

For subjects with MS, the T1W-SE and GEPCI sequences were repeated after injection of a gadolinium-based contrast agent. None of the 5 subjects with MS had gadolinium-enhancing lesions.

Generating GEPCI Images

Magnitude and phase images as well as raw data are stored for data analysis. Image reconstruction and post-processing are performed using a standard PC computer and Matlab software (MathWorks Inc.). The MR signal derived from the multi-gradient echo imaging experiment has contributions from both tissue-specific microscopic and mesoscopic field inhomogeneities, and also from macroscopic field inhomogeneities (Yablonskiy 1998). Macroscopic field inhomogeneities arise from magnet imperfections, body-air interfaces, large sinuses inside of the body etc. These field inhomogeneities lead to effects such as signal loss and image distortion and may compromise tissue matrix quantification if not properly recognized. We have previously shown (Yablonskiy 2000a; Yablonskiy 2000b; Yablonskiy 2003) that the GEPCI signal *S(TE)* at a gradient echo time TE from a given voxel can be represented as a product of signal that would exist in the absence of macroscopic field inhomogeneities, multiplied by the function *F(TE)* that represents relative signal attenuation caused by macroscopic field inhomogeneities:

$$S(TE)=S(0)\cdot\exp(-R2*\cdot TE)\cdot F(TE) \quad [1]$$

Where R2* is the relaxation rate constant that has only tissue-specific contributions from both microscopic, R2, and mesoscopic, R2′, relaxations (R2* = R2 + R2′).

If *F(TE)* is known, Eq. [1] can be fitted to data on a voxel-by-voxel basis to obtain R2* and *S*(0) maps that are not contaminated by macroscopic field inhomogeneities. Depending on the sequence parameters, the map of *S*(0) represents either a T1 or spin-density weighted image. In our protocol, a short TR and large flip angle are selected to obtain S(0) as a T1-weighted image.

Additional quantitative FLAIR-like images can be generated from GEPCI-T2* maps. After manually segmenting out the skull, voxels corresponding to cerebrospinal fluid (CSF) in T1W-GEPCI images can be identified using a threshold based on T1W intensity. This procedure is possible because CSF has a T1 relaxation time constant that is significantly different from gray matter (GM) and WM providing an excellent contrast in the T1W-GEPCI image. A mask of the remaining brain tissue voxels (without CSF) is then applied to the GEPCI-T2* map. The resulting GEPCI-T2* map is called a GEPCI-FLAIR image.

Fifteen imaging slices covering most of the cerebral white matter were used for data analysis for each subject. Our data demonstrate that the automatic shimming procedure available on Siemens scanner allows substantial minimization of macroscopic field inhomogeneity effects. We found that with our 3D high-resolution GEPCI approach, the deviation of the function *F(TE)* from unity is negligible in most parts of the brain important for MS. Hence, a simple fitting of the monoexponential function in Eq. [1] with *F(TE)* = 1 to the GEPCI signal is sufficient to generate GEPCI images. Such an approach was used in the study we describe here; however, in the areas of the brain close to sinuses this correction is required. This correction might also be needed for applications at higher field strength. It can be done by using MR signal frequency shift available from complex data set generated by GEPCI technique. Corresponding methods were previously discussed by us (Yablonskiy 1998; Yablonskiy 2003).

Scoring method of Multiple Sclerosis severity

Each MS lesion voxel in GEPCI technique is characterized by an associated quantitative T2* relaxation time constant. We hypothesize that the R2* relaxation rate constant (R2*=1/T2*) will provide information on lesion severity. This hypothesis is a natural step because MS tissue damage involves loss of myelin lipids accompanied to variable degree by loss of intracellular proteins, including axon proteins. In this process, R2* relaxation rate constant will progressively decrease from normal tissue values to values typical for interstitial fluid or CSF that is practically devoid of macromolecules. This supposition is in agreement with correlation established between tissue T1 and T2 values and tissue damage in MS reported in (Schmierer et al. 2008; Seewann et al. 2009). Recall, that R2* = R2 +R2′, where R2=1/T2 and R2′ reflects contribution from mesoscopic field inhomogeneities generated mostly by the presence of blood vessel network in the brain tissue (Yablonskiy 1998). Recent work has evaluated the tissue-specific R2′ relaxation rate in the healthy human brain (He and Yablonskiy 2007). Using this data, we found R2′ value for white matter at 1.5T to be equal to 0.35 s^{-1}, and at 3T it is 0.7 s^{-1}, both are much smaller compared with the typical WM R2 value that is approximately equal to 15-16 s^{-1} (Neema et al. 2009). The GEPCI technique, therefore, provides a quantitative measure of a tissue-specific relaxation time T2* (equal to 1/R2*) that is very close to T2 measured using spin-echo sequences. Based on this consideration, we adopted the following procedure for estimation and scoring of tissue damage in MS:

The first step of the scoring method is the design of the masks which contain only white matter, including both normal-appearing and lesioned areas. Herein these masks are drawn manually on T1W-GEPCI images using home-built Matlab programs. All gray matter structures (cortical and deep) are excluded. Masks are applied on both T1W-GEPCI images and GEPCI-T2* maps. Then R2* histograms (Fig.5 jkl) of the voxels inside masks of all fifteen slices are generated using a bin width of 0.3 s^{-1} ranging from 0 s^{-1} up to 30 s^{-1}. For control subjects these histograms look almost like ideal Gaussian distributions. For subjects with MS these histograms have a large peak with a quasi-Gaussian shape [corresponding to normal appearing white matter (NAWM)] and a strongly elevated non-Gaussian tail on the left resulted from the presence of the MS lesions (see examples in the Results section).

The next step is to define the level of tissue damage, or *tissue damage score* (TDS), for each voxel in MS lesions. To perform this calculation, we define a *damage scale* based on the tissue R2* value. The characteristics of the WM peak are determined using a standard Gaussian function that is fitted to the R2* distribution. To remove any influence on the fit from the tail existing in the R2* distribution of MS patients, we fit only the upper half of the R2* histogram. We define the "normal reference" R2* value as corresponding to the center of the NAWM peak ($R2^*_c$) obtained from the fitting procedure. As we already mentioned, in MS, tissue damage occurs through the loss of macromolecules, mainly myelin and proteins in axons, leading to reduction in tissue R2*. Hence, for each voxel in MS lesion with a given R2* value, the tissue damage score (TDS) is determined as:

$$TDS = \frac{R2^*_c - R2*}{R2^*_c} \quad [2]$$

In addition to defining TDS for each voxel, we can also define the *tissue damage load* (TDL) for a given patient. This is done by summing TDS over all the voxels in MS lesions:

$$TDL = V \cdot \sum_{i=1:N} TDS_i \quad [3]$$

where N represents the total number of voxels in the MS lesions in cerebral white matter. We have also multiplied the sum by the voxel volume V (mm^3) to make this definition independent on the voxel resolution of the MRI pulse sequence. The tissue damage load, thus, assesses both the lesion load *and* the degree of severity of the MS lesions. Additionally, a *mean tissue damage score* (MTDS) can also be obtained by averaging TDS over all the lesions:

$$MTDS = \left(\sum_{i=1:N} TDS_i \right) / N \quad [4]$$

This mean score provides an estimate of the average severity of abnormal white matter tissue in the subject's brain.

To apply Eqs. [3] and [4], we need to define a method for separating "normal" brain tissue from MS lesions. This procedure is always ambiguous because lesions almost never have sharp boundaries. Also, the distribution function of R2* values of normal WM has a Gaussian type shape. As for any Gaussian distribution, 95% of R2* values are located around peak center in

the interval $R2* = R2_c^* \pm 1.96\sigma$, and 99% of values are in the interval $R2* = R2_c^* \pm 2.58\sigma$, where σ is the distribution width. This means that even in the normal brain there are voxels that have "abnormal" GEPCI scores. Hence separation of tissue into "normal" and "abnormal" is always somewhat subjective. Visual examination by neurologist (A.H.C.) of GEPCI and standard clinical images from subjects with MS suggested that the threshold of 1.96σ separates most of the MS lesions from normal-appearing tissue. We will use this threshold in this pilot study leaving more detailed examination for future work. In addition, all the voxels that have R2* below selected threshold and are isolated (single voxels) or have only one neighbor (hanging voxels) are eliminated from consideration to reduce influence of noise on our quantitative estimates.

Statistical Analyses

Statistical analyses were performed with JMP Statistical Software Release 8.0.1 (SAS Institute, Inc., Cary, NC) and MedCalc Statistics for Biomedical Research Version 10.3.0.0 (MedCalc Software, Mariakerke, Belgium). Normal curves were fitted to data distributions and the normality of the distributions tested with the Shapiro-Wilk W test. Equality of variances was tested with the O'Brien, Brown-Forsythe, Levene, and Bartlett tests. Differences between MS and control subjects groups were tested with the Student's t test and 95% confidence intervals were calculated. Alpha was set at 0.05. As data distributions for TDL and MTDS were non-normal (Shapiro-Wilk W test, $P < 0.05$), Spearman rank correlations coefficients were calculated between EDSS and LL (mm^3), TDL (mm^3) and MTDS.

Results

Typical signal-to-noise ratio (SNR) in the image corresponding to first gradient echo is about 40. Figure 2 shows the images obtained with GEPCI of a healthy control subject. Tissue delineation is similar between images obtained with GEPCI and SE images--all types of contrast that are seen with SE sequences are revealed with GEPCI as well; however the gray-white-matter contrast is substantially improved with T1W-GEPCI (Figure 2d) as compared to T1W-SE (Figure 2a).

Figure 3 shows the images obtained with GEPCI of a subject with RRMS (MS #3). Again, tissue delineation is similar between GEPCI and SE images, with identical lesion distribution. MS lesion contrast is well resolved with GEPCI (hypointense on T1W image and hyperintense on T2* map), thus allowing standard identification of MS lesions. In addition, similar lesion distribution is observed between GEPCI and standard SE imaging.

Images obtained with GEPCI of a subject (MS #5) with SPMS (Figure 4) also show the same lesion distribution as compared to SE images. Note that this subject with SPMS has a higher lesion load than the subject with RRMS, and multiple "black holes" are present in the T1-weighted images (Figures 4a and 4d). Several MS lesions are as hyperintense as cerebrospinal fluid on T2W-SE image (Figure 4b) and display T2* times similar to CSF on GEPCI-T2* map (Figure 4e); this suggests very severe (cystic) lesions. Indeed, these 'lesions' have some properties similar to CSF, and as a consequence they are suppressed on both standard FLAIR image (Figure 4c) and GEPCI-FLAIR image (Figure 4f).

As we discussed, T2W SE images and GEPCI T2* maps display rather common features. While we do not expect quantitative correlation between these images, we do expect certain association between them, as shown in Fig. 5 for the same subject as in Fig. 4 (MS#5).

Scoring the severity of multiple sclerosis tissue damage using GEPCI

Here, the successive steps of the proposed scoring method are illustrated with the three subjects introduced previously. Examples of the initial and resulting T1W-GEPCI images after application of the WM masks are provided in Figure 6 (Figure 6 a, b and c for initial images, and Figure 6 d, e and f for resulting images). The 3D histograms of segmented voxels belonging to WM and MS lesions (or WM only for controls) are displayed in Figure 6 g, h and i based on their R2* relaxation rate values and their T1W image intensities obtained with GEPCI. From these histograms, one can observe marked differences in the distributions for the three subjects. The healthy control displays a Gaussian distribution corresponding to a range of "normal" R2* values and T1W intensities of WM. The distribution for the subject with RRMS (MS #3) has an additional "abnormal" tail of voxels with lower R2* and T1W values. For the subject with SPMS (MS #5), the alteration of the normal Gaussian distribution is even greater as the tail contains more voxels with lower R2* and T1W values. These 3D histograms provide information on both T1W intensity and R2* relaxation rate constant for tissue represented in the images obtained with GEPCI. However, T1W intensity depends not only on tissue properties but also on the MRI pulse sequence parameters and RF coil sensitivity. On the other hand, the R2* value is a tissue specific parameter, independent of pulse sequence if properly evaluated (Yablonskiy 1998;Yablonskiy 2000a;Yablonskiy 2000b). Hence, we use the R2* parameter and its associated histogram to develop our quantitative scoring method.

An illustration of the scores obtained for the subjects with RRMS and SPMS is provided in Figure 7. Lesions on images were identified by our neurologist (A.H.C.). The tissue damage score of each abnormal voxel was then calculated using Eq. [2]. In this figure, the abnormal voxels, which define the lesion areas in the slice of interest, are colored and overlaid on the T1W-GEPCI images. Colors correspond to a score ranging from 0 to 1 and represent the level of tissue damage. The magnified view of the lesions for the subject with RRMS shows scores in the blue color range which indicate low severity of tissue damage. On the other hand, the magnified view of the lesions for the subject with SPMS displays many scores with the red color indicating very severe tissue damage.

The R2* distribution for the healthy control has a symmetric peak with excellent matching between the Gaussian fitted line and the R2* distribution (Figure 6j). As with the 3D histograms, the R2* histograms for the subjects with MS display tails of voxels with lower R2* values on the left of the NAWM peak and with higher R2* values on the right. For the two subjects with MS (Figures 6k and 6l), mismatches between the Gaussian fitted lines and the distributions are seen in the tails. The fitting results obtained for Gaussian peak center and peak width are reported in Table 1 for normal control subjects and subjects with MS. The tissue damage load and the mean tissue damage score were calculated using Eqs. [3] and [4] and are shown in the table. The clinical disability score (EDSS) for each MS subject is also included in Table 1. All three MR markers (lesion load, TDL and MTDS) increased in graded fashion from subject #1 up to subject #5, indicating a progressive increase in the load and the severity of the MS lesions. Similarly, the EDSS score increased in a graded fashion from subject #1 to subject #5, indicating the progressive increase in the severity of the MS disease.

The results of fitting and scoring analysis for healthy control subjects, shown in Table 1, were used to define statistical distribution of corresponding parameters for control group. Based on these distributions we estimated corresponding differences in MS subjects.

Discussion

Conventional MRI findings based on standard SE sequences do not correlate well with the severity of the disease assessed by clinical testing. This lack of correlation is often referred to as the "MRI paradox" (Mainero et al. 2001; Brex et al. 2002; Sormani et al. 2003). While this

paradox can be attributed in part to the complexity of the underlying tissue damage in MS and to the different functional effects based on different lesion locations, the paradox might also be caused in part by lack of quantitative information about the severity of tissue damage in MS lesions using standard MRI protocols. This last shortcoming can be overcome with a relaxometry approach such as the GEPCI technique introduced by our laboratory. GEPCI is a simple yet robust technique allowing acquisition of quantitative T2* and FLAIR-like maps, along with T1-weighted images in a single scan within a clinically acceptable time frame. In this study, we demonstrated several advantages of GEPCI over SE sequences for standard evaluation of MS. *First*, images obtained with GEPCI appear highly similar to standard scans; hence, they can be used in a reliable and conventional way for a clinical evaluation of the disease. *Second*, T1W-GEPCI images, GEPCI-T2* maps and GEPCI-FLAIR maps are generated from a single dataset; hence, they are inherently co-registered. *Third*, the GEPCI technique is based on gradient-echo MRI and uses small flip angles as compared to spin-echo based techniques; hence it can be safely used in high-field MRI. *Fourth*, the acquisition time for simultaneous generation of these three images is considerably reduced compared with their equivalent SE sequences (8 min 32 s for GEPCI against a total of 16 min scanning time for three scans in a standard clinical protocol). However, the main advantage of GEPCI approach is its quantitative nature (T2* relaxometry) which we use to evaluate the severity of MS tissue damage based on the scoring method introduced in this paper.

Table 1 shows results for tissue damage load (TDL), mean TDS (MTDS) and lesion load (LL), to summarize 3D GEPCI data from cerebral white matter of 5 healthy controls and 5 MS subjects, respectively. Data of interest not only include the TDL determined by the “tail” of low R2* values located outside 1.96 sigma from peak center, but also the peak widths and center in the distribution of the R2* relaxation rate constants. Note in the table of data from MS subjects that all quantitative GEPCI indexes - the TDL, the LL, and the MTDS were highly correlated with the EDSS. However, it is possible that these correlation coefficients are artificially “good”, due to the large EDSS range of the small number of MS subjects examined.

Using R2* histograms to assess global changes in the whole brain, we showed that normal white matter from healthy controls displays a practically Gaussian distribution of R2* values. For subjects with MS, the distributions have elevated tails of abnormal voxels at lower R2* values. These abnormal voxels correspond to areas of MS lesions. Our data suggest that the tails appear larger and more skewed as the lesion load and underlying tissue damage increase. Thus, we hypothesize that the progressive demyelination and axonal loss that occur during MS evolution result in an increased number of abnormal voxels having a reduced R2* relaxation rate constant reflecting reduced tissue integrity (R2* is proportional to macromolecule concentration). This hypothesis is supported by studies of *post-mortem* brain MS tissues (Schmierer et al. 2008; Seewann et al. 2009) that found strong correlations between MS pathologies and T2, and T1, relaxation times. A similar correlation should exist for T2* relaxation time, as this relaxation mechanism combines properties of T2 relaxation with a small contribution from mesoscopic field inhomogeneities originating mostly from deoxyhemoglobin in the blood. Hence, T2* might be even more informative parameter than T2. Due to very low blood volume fraction in WM (about 1-2%), the T2* values of WM are, however, similar to their T2 values (He and Yablonskiy 2007).

As previously discussed, Neema et al (Neema et al. 2009) and Parry et al (Parry et al. 2002) proposed quantitative T2 and T1 techniques for evaluating of changes in MS tissue. While these techniques are faster as compared to CPMG-based method used in (Papanikolaou et al. 2004), it would still require more than half an hour imaging time to obtain images of the same resolution (256 × 256) as we obtain by GEPCI in about 8 minutes.

We introduced three new quantitative parameters to score the severity of the disease, based on the T2* (or R2*) changes in MS lesions,: 1) The *tissue damage load* which combines both volume and severity of abnormal white matter; 2) The *mean tissue damage score* which provides an average severity of abnormal tissue, perhaps indicating the aggressiveness of the disease; and 3) The *tissue damage score* which assesses the level of brain tissue damage at the voxel level, and is based on the normalized difference between tissue R2* and the R2* value for NAWM. The underlying hypothesis is that reduction in R2* value (increase in T2* value) would reflect worsening of MS pathology due to demyelination, axonal loss and increased extracellular water content. Therefore, a R2* value close to CSF corresponds to the worst severity. This is notably supported by a previous study (Rovaris et al. 1999) where MS lesions suppressed by the FLAIR sequence were areas of severe tissue damage. Hence, we propose that the TDS might reflect severity of tissue damage at the voxel level in MS lesions. We should also note that there is no “clear boundary” between different levels of tissue damage. Also important is the question of the threshold GEPCI-defined values for detecting mildly affected white matter (either normal-appearing or “dirty” WM) which is also believed to contribute to the development of clinical disability in MS patients (Kutzelnigg et al. 2005).

Underlying tissue pathology in MS is often complicated and changes in the R2* relaxation rate constant reflect only global changes in the tissue microstructure, mostly reflecting diminished macromolecular content. Thus, an apparent loss of macromolecular content might be seen in situations when extra-fluid is present in otherwise normal tissue. For example, for gadolinium-enhancing lesions, there might be an overestimation of tissue damage due to a temporary increase in water content during the blood-brain-barrier (BBB) breakdown event (Katz et al. 1993). This effect might potentially reduce R2* even more than would non-enhancing lesions with a similar level of tissue damage. Although none of the 5 subjects in the present study had gadolinium-enhancing lesions, future longitudinal studies will investigate the effect of BBB breakdown, reflected by gadolinium-enhancement, on tissue damage score.

Our scoring method allows inter-patient comparisons. As our current calculation of the tissue damage score is based on the R2* change relative to the R2* value of the peak center and is normalized to the peak center (see Eq.[2]), it is practically immune to variation in the position of peak center. However, this approach excludes information that might come from the peak position itself. Recent publications based on T1 and T2 relaxometry suggest that the characteristics of the NAWM peak also contain information about the disease (Vrenken et al. 2006; Neema et al. 2009) (Parry et al. 2002). More particularly, a significant shift of the normal white matter peak position and a significant increase of its width were observed by comparing patients with MS with age- and gender-matched healthy controls. Both phenomena were suggested to stem from pathologies in NAWM. In our study, we also observed similar differences between healthy controls and subjects with MS although a small sample size does not allow us to reach significant conclusions (see Table 1). Perhaps biological effects due to age also contributed in our study, as the subjects with MS and control subjects were not fully age-matched. This will be a subject of future studies.

Finally, although the results obtained in this pilot study are promising, the MRI scans were performed on a limited part of the CNS (cerebrum only), and were performed on a small number of subjects. Therefore, the strong correlation between the results of our scoring method and the disability scores should be taken with caution. Future studies will enroll a larger MS cohort, to better assess the sensitivity of this novel imaging method over conventional imaging methods. Correlations should also be investigated at the regional level to take into account the lesion location factor. Note that cortical gray matter could be investigated in the same manner as white matter since similar phenomenon were observed in T1 histograms from normal appearing gray matter of patients with MS (Vrenken et al. 2006).

In this paper we developed a tissue-damage scoring system based on quantitative R2* histograms obtained by means of the GEPCI technique. A similar scoring method can be developed based on quantitative T1 and T2 measurements. Moreover, because the MR relaxation rate constants R1 and R2 are expected to depend linearly on tissue damage, similar to the R2* relaxation rate constant, we might expect that normalized scores (TDS, TDL and MTDS) could be similar for all three methods. Hence, different relaxometry techniques could be used for collecting quantitative scoring maps.

In summary, this pilot study using a 1.5T MRI scanner shows that a multi-gradient-echo GEPCI technique derives images similar to SE sequences in a clinically acceptable time, shorter than current clinical protocols, and can be used for an advanced evaluation of tissue damage due to MS. This study also introduces for the first time a MRI-based scoring method for MS using R2* relaxometry. This method is sensitive not only to lesion load, but also to the degree of damage within the MS lesions. This method holds promise for improving the quantitative evaluation of MS pathology, both in the clinic and as a research tool.

Acknowledgments

The authors would like to thank Gayla Gregory R.N. for assistance with the patients, Kevin Cross and Cecile Sati for helping with data processing, Linda Hood and Richard Nagel for helping with MRI scanning, Dr. Adil Bashir for technical support with the pulse sequence, and the subjects with MS and healthy volunteers for their time. Dr. Cross was supported in part by the Manny and Rosalyn Rosenthal- Dr. John L. Trotter Chair in Neuroimmunology of Barnes-Jewish Hospital Foundation. This publication was made possible by Grant Number UL1 RR024992 from the National Center for Research Resources (NCRR), a component of the National Institutes of Health (NIH).

References

Barbosa S, Blumhardt LD, Roberts N, Lock T, Edwards RH. Magnetic resonance relaxation time mapping in multiple sclerosis: normal appearing white matter and the “invisible” lesion load. Magn Reson Imaging 1994;12(1):33–42. [PubMed: 8295506]

Barkhof F, McGowan JC, van Waesberghe JH, Grossman RI. Hypointense multiple sclerosis lesions on T1-weighted spin echo magnetic resonance images: their contribution in understanding multiple sclerosis evolution. J Neurol Neurosurg Psychiatry 1998;64:S77–9. [PubMed: 9647290]

Barkhof F, van Walderveen M. Characterization of tissue damage in multiple sclerosis by nuclear magnetic resonance. Philos Trans R Soc Lond B Biol Sci 1999;354(1390):1675–86. [PubMed: 10603619]

Bashir A, Cross AH, Yablonskiy DA. Gradient Echo Plural Contrast Imaging for Evaluating Multiple Sclerosis. Proceedings of ISMRM. 2007

Bashir A, Yablonskiy DA. Gradient Echo Plural Contrast Imaging (GEPCI). Proceedings of ISMRM. 2006

Bjartmar C, Wujek JR, Trapp BD. Axonal loss in the pathology of MS: consequences for understanding the progressive phase of the disease. J Neurol Sci 2003;206(2):165–71. [PubMed: 12559505]

Brex PA, Ciccarelli O, O'Riordan JI, Sailer M, Thompson AJ, Miller DH. A longitudinal study of abnormalities on MRI and disability from multiple sclerosis. N Engl J Med 2002;346(3):158–64. [PubMed: 11796849]

Chitnis T, Pirko I. Sensitivity vs specificity: progress and pitfalls in defining MRI criteria for pediatric MS. Neurology 2009;72(11):952–3. [PubMed: 19289735]

Fulton JC, Grossman RI, Udupa J, Mannon LJ, Grossman M, Wei L, Polansky M, Kolson DL. MR lesion load and cognitive function in patients with relapsing-remitting multiple sclerosis. AJNR Am J Neuroradiol 1999;20(10):1951–5. [PubMed: 10588124]

Grenier D, Pelletier D, Normandeau M, Newitt D, Nelson S, Goodkin DE, Majumdar S. T2 relaxation time histograms in multiple sclerosis. Magn Reson Imaging 2002;20(10):733–41. [PubMed: 12591569]

He X, Yablonskiy DA. Quantitative BOLD: mapping of human cerebral deoxygenated blood volume and oxygen extraction fraction: default state. Magn Reson Med 2007;57(1):115–26. [PubMed: 17191227]

Katz D, Taubenberger JK, Cannella B, McFarlin DE, Raine CS, McFarland HF. Correlation between magnetic resonance imaging findings and lesion development in chronic, active multiple sclerosis. Ann Neurol 1993;34(5):661–9. [PubMed: 8239560]

Kurtzke JF. Rating neurologic impairment in multiple sclerosis: an expanded disability status scale (EDSS). Neurology 1983;33(11):1444–52. [PubMed: 6685237]

Kutzelnigg A, Lucchinetti CF, Stadelmann C, Bruck W, Rauschka H, Bergmann M, Schmidbauer M, Parisi JE, Lassmann H. Cortical demyelination and diffuse white matter injury in multiple sclerosis. Brain 2005;128(Pt 11):2705–12. [PubMed: 16230320]

Lublin FD, Reingold SC. Defining the clinical course of multiple sclerosis: results of an international survey. National Multiple Sclerosis Society (USA) Advisory Committee on Clinical Trials of New Agents in Multiple Sclerosis. Neurology 1996;46(4):907–11. [PubMed: 8780061]

Lucchinetti C, Bruck W, Parisi J, Scheithauer B, Rodriguez M, Lassmann H. Heterogeneity of multiple sclerosis lesions: implications for the pathogenesis of demyelination. Ann Neurol 2000;47(6):707–17. [PubMed: 10852536]

Mainero C, De Stefano N, Iannucci G, Sormani MP, Guidi L, Federico A, Bartolozzi ML, Comi G, Filippi M. Correlates of MS disability assessed in vivo using aggregates of MR quantities. Neurology 2001;56(10):1331–4. [PubMed: 11376183]

Neema M, Goldberg-Zimring D, Guss ZD, Healy BC, Guttmann CR, Houtchens MK, Weiner HL, Horsfield MA, Hackney DB, Alsop DC, Bakshi R. 3 T MRI relaxometry detects T2 prolongation in the cerebral normal-appearing white matter in multiple sclerosis. Neuroimage 2009;46(3):633–41. [PubMed: 19281850]

Papanikolaou N, Papadaki E, Karampekios S, Spilioti M, Maris T, Prassopoulos P, Gourtsoyiannis N. T2 relaxation time analysis in patients with multiple sclerosis: correlation with magnetization transfer ratio. Eur Radiol 2004;14(1):115–22. [PubMed: 14600774]

Parry A, Clare S, Jenkinson M, Smith S, Palace J, Matthews PM. White matter and lesion T1 relaxation times increase in parallel and correlate with disability in multiple sclerosis. J Neurol 2002;249(9):1279–86. [PubMed: 12242554]

Rovaris M, Comi G, Rocca MA, Cercignani M, Colombo B, Santuccio G, Filippi M. Relevance of hypointense lesions on fast fluid-attenuated inversion recovery MR images as a marker of disease severity in cases of multiple sclerosis. AJNR Am J Neuroradiol 1999;20(5):813–20. [PubMed: 10369351]

Sati, P.; Cross, AH.; Bashir, A.; Yablonskiy, DA. Evaluation of multiple sclerosis lesions using gradient echo plural contrast imaging. World Congress on Treatment and Research in Multiple Sclerosis; Montreal: 2008a.

Sati, P.; Cross, AH.; Bashir, A.; Yablonskiy, DA. Gradient Echo Plural Contrast Imaging: A Novel MRI Technique for Evaluating Multiple Sclerosis; 94th Annual Meeting of Radiological Society of North America Chicago; 2008b.

Sati, P.; Cross, AH.; Schmidt, R.; Yablonskiy, D. Advantages of Gradient Echo Plural Contrast Imaging for Identifying MS Abnormalities in Postmortem Brain Tissue; 17th Annual Meeting of the International Society for Magnetic Resonance in Medicine; Honolulu. 2009a.

Sati, P.; Cross, AH.; Schmidt, RE.; Yablonskiy, DA. In-vivo and ex-vivo evaluation of Multiple Sclerosis lesions using Gradient Echo Plural Contrast Imaging. Keystone Symposium on Multiple Sclerosis; Santa Fe: 2009b.

Sati, P.; Cross, AH.; Yablonskiy, DA. In-vivo Quantitative Measure of Black Hole Severity in Multiple Sclerosis with Gradient Echo Plural Contrast Imaging; 17th Annual Meeting of the International Society for Magnetic Resonance in Medicine; Honolulu. 2009c.

Schmierer K, Wheeler-Kingshott CA, Tozer DJ, Boulby PA, Parkes HG, Yousry TA, Scaravilli F, Barker GJ, Tofts PS, Miller DH. Quantitative magnetic resonance of postmortem multiple sclerosis brain before and after fixation. Magn Reson Med 2008;59(2):268–77. [PubMed: 18228601]

Seewann A, Vrenken H, van der Valk P, Blezer EL, Knol DL, Castelijns JA, Polman CH, Pouwels PJ, Barkhof F, Geurts JJ. Diffusely abnormal white matter in chronic multiple sclerosis: imaging and histopathologic analysis. Arch Neurol 2009;66(5):601–9. [PubMed: 19433660]

Sicotte NL, Voskuhl RR, Bouvier S, Klutch R, Cohen MS, Mazziotta JC. Comparison of multiple sclerosis lesions at 1.5 and 3.0 Tesla. Invest Radiol 2003;38(7):423–7. [PubMed: 12821856]

Simon JH. MRI in multiple sclerosis. Phys Med Rehabil Clin N Am 2005;16(2):383–409. viii. [PubMed: 15893678]

Sormani MP, Bruzzi P, Beckmann K, Wagner K, Miller DH, Kappos L, Filippi M. MRI metrics as surrogate endpoints for EDSS progression in SPMS patients treated with IFN beta-1b. Neurology 2003;60(9):1462–6. [PubMed: 12743232]

Stevenson VL, Parker GJ, Barker GJ, Birnie K, Tofts PS, Miller DH, Thompson AJ. Variations in T1 and T2 relaxation times of normal appearing white matter and lesions in multiple sclerosis. J Neurol Sci 2000;178(2):81–7. [PubMed: 11018698]

Traboulsee A, Li DK. Conventional MR imaging. Neuroimaging Clin N Am 2008;18(4):651–73. x. [PubMed: 19068407]

Vaithianathar L, Tench CR, Morgan PS, Lin X, Blumhardt LD. White matter T(1) relaxation time histograms and cerebral atrophy in multiple sclerosis. J Neurol Sci 2002;197(1-2):45–50. [PubMed: 11997065]

van Walderveen MA, Kamphorst W, Scheltens P, van Waesberghe JH, Ravid R, Valk J, Polman CH, Barkhof F. Histopathologic correlate of hypointense lesions on T1-weighted spin-echo MRI in multiple sclerosis. Neurology 1998;50(5):1282–8. [PubMed: 9595975]

Vrenken H, Geurts JJ, Knol DL, van Dijk LN, Dattola V, Jasperse B, van Schijndel RA, Polman CH, Castelijns JA, Barkhof F, Pouwels PJ. Whole-brain T1 mapping in multiple sclerosis: global changes of normal-appearing gray and white matter. Radiology 2006;240(3):811–20. [PubMed: 16868279]

Yablonskiy DA. Quantitation of intrinsic magnetic susceptibility-related effects in a tissue matrix. Phantom study. Magn Reson Med 1998;39(3):417–28. [PubMed: 9498598]

Yablonskiy DA. Gradient echo plural contrast imaging (GEPCI) - New fast magnetic resonance imaging technique for simultaneous acquisition of T2, T1 (or spin density) and T2*-weighted images. Radiology 2000a;217:21.

Yablonskiy, DA. Quntitative T2 contrast with Gradient Echoes. 8th Annual Meeting of the International Society for Magnetic Resonance in Medicine Denver; Colorado. 2000b.

Yablonskiy, DA. T2 Contrast with Gradient Echoes. USA Patent 6603989. 2003.

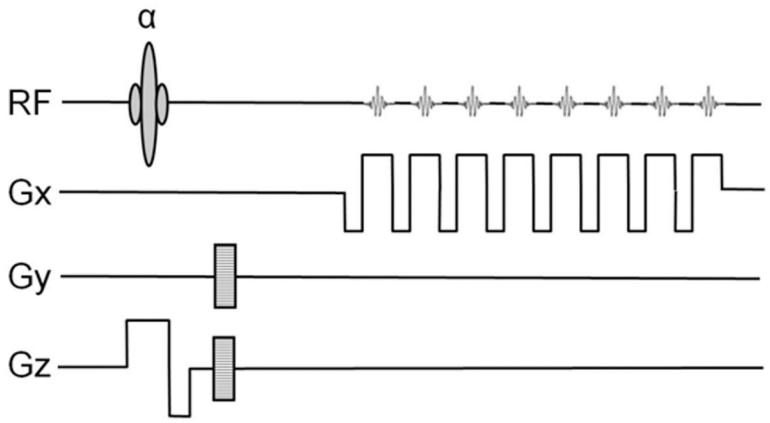

Figure 1.
Schematic structure of GEPCI pulse sequence diagram. Upper lane is the RF pulse α and multiple gradient echoes. Gx is the structure of read-out magnetic field gradients. Gy represents in-plane phase encoding gradients. Gz is designed for slice selection and in-slice phase encoding (3D version).

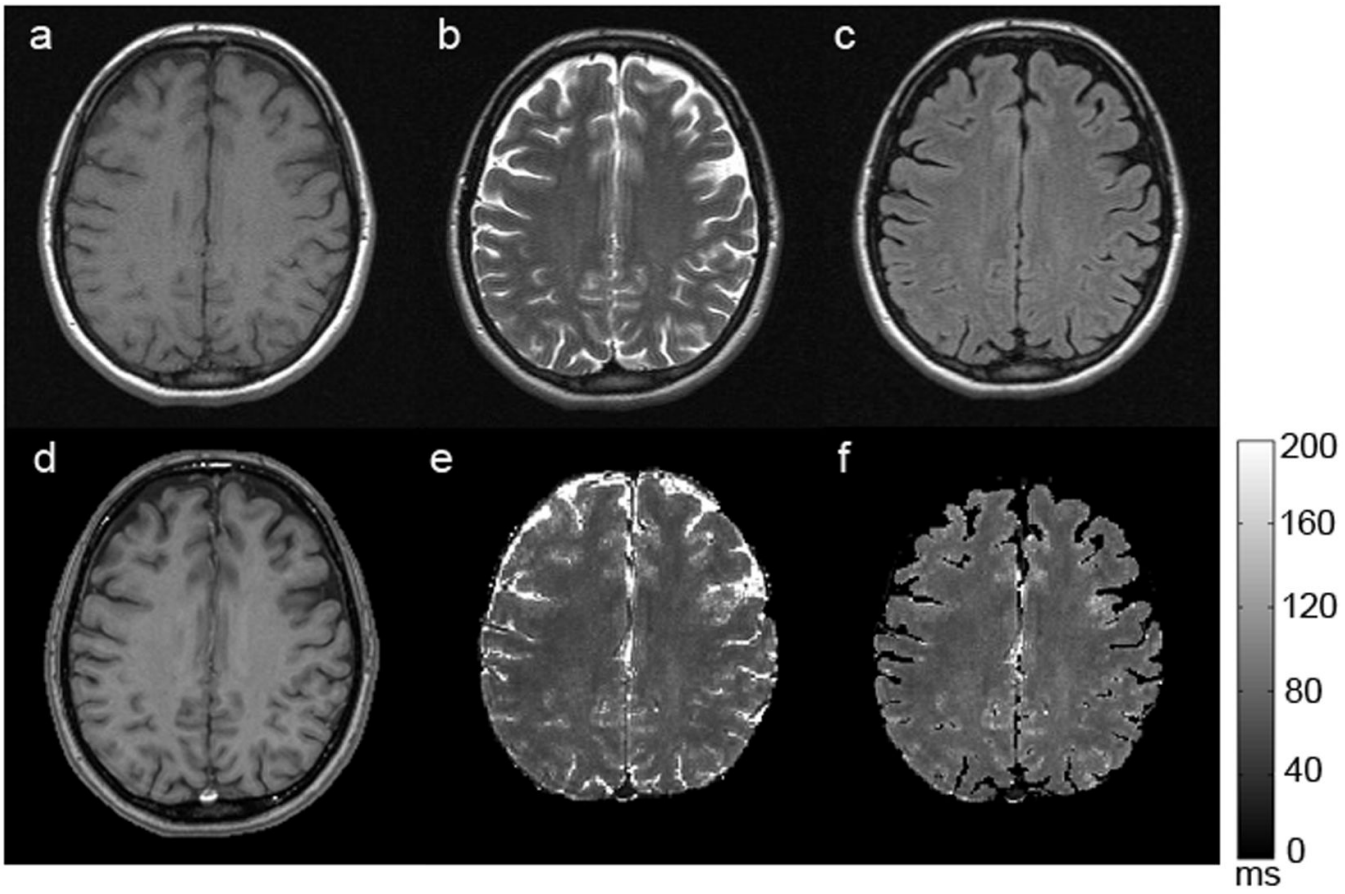

Figure 2.

A representative set of images obtained from a healthy volunteer. The upper row represents standard TSE images: a) T1W-SE, b) T2W-SE, c) T2W-FLAIR; The bottom row represents corresponding images obtained with the GEPCI approach: d) T1W-GEPCI, e) GEPCI-T2* map, f) GEPCI-FLAIR image. The scale bar shows the T2* relaxation time constant in milliseconds.

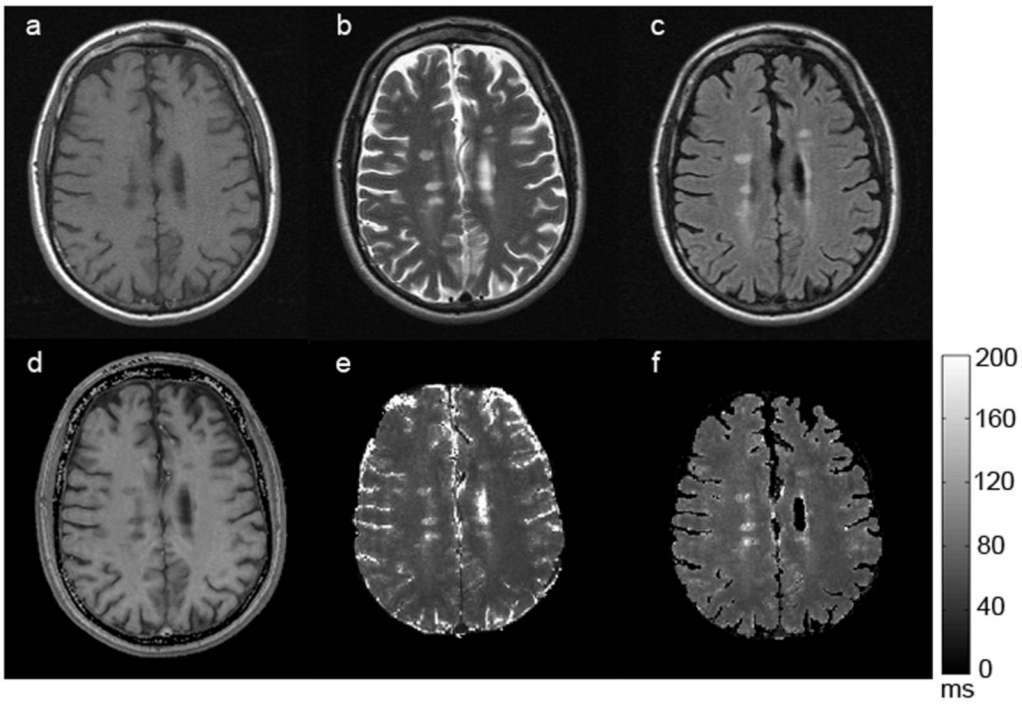

Figure 3.

A representative set of images obtained from a subject (MS #3) with RRMS. The upper row represents standard TSE images: a) T1W-SE, b) T2W-SE, c) T2W-FLAIR; The bottom row represents corresponding images obtained with the GEPCI approach: d) T1W-GEPCI, e) GEPCI-T2* map, f) GEPCI-FLAIR image. The scale bar shows T2* relaxation time constant in milliseconds.

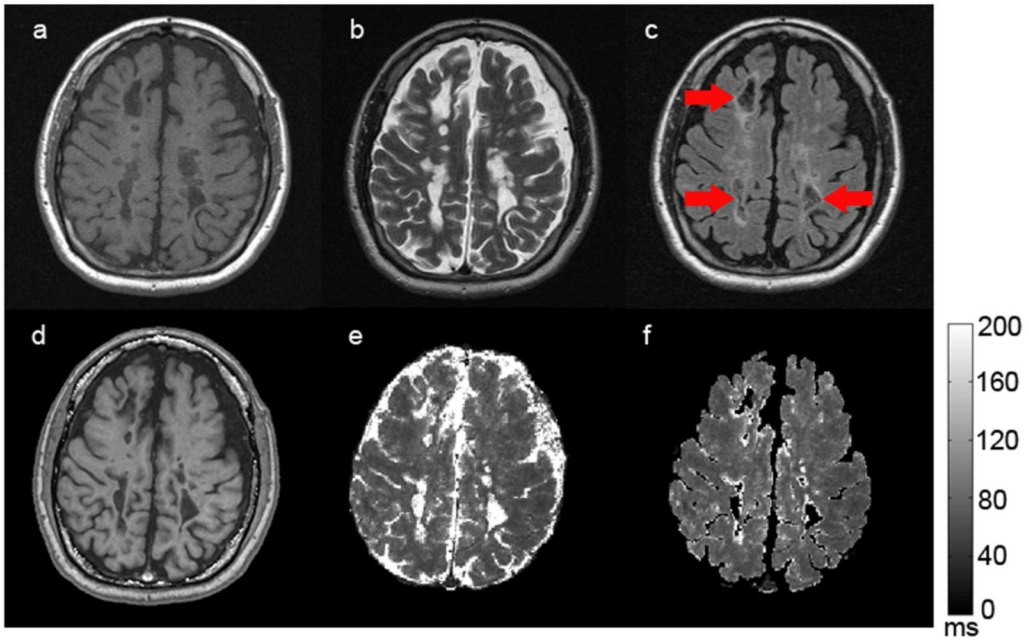

Figure 4.

A representative set of images obtained from a subject (MS #5) with SPMS. The upper row represents SE images: a) T1W-SE, b) T2W-SE, c) T2W-FLAIR; The bottom row represents corresponding images obtained with the GEPCI approach: d) T1W-GEPCI, e) GEPCI-T2* map, f) GEPCI-FLAIR image. The scale bar shows the T2* relaxation time constant in milliseconds. Cystic lesions suppressed on FLAIR images are indicated by red arrows.

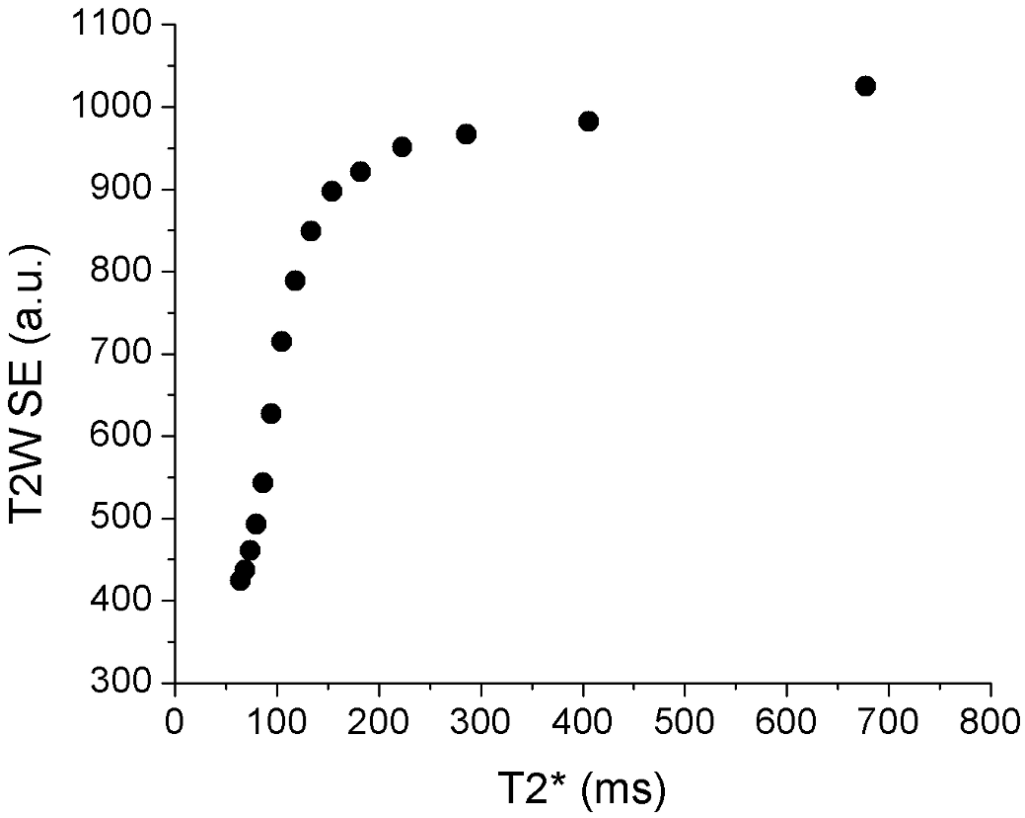

Figure 5.

Association between T2W SE images and GEPCI T2* maps. While Figs. 2-4 show that GEPCI-T2* maps highly resemble the T2W-SE images, the linear relationships between signal intensity in T2W images and corresponding GEPCI T2* relaxation time constants is not expected. Yet certain association between these parameters does exist. The plot displays the relationship between T2* values and the intensity of T2W image. Pixels from white matter on co-registered T2* maps and T2 weighted images were divided into 15 groups by their R2* values ranging from R2*= 1 s^{-1} to R2* = 16 s^{-1} (corresponding to the peak center in the subject #5). Each point in the plot represents mean value for the corresponding group. As the plot shows, the T2* and T2W intensity grow proportionally when T2* is below 150ms. However, the T2W intensity reaches plateau for mild and severe lesions while T2* still varies substantially, thus offering better delineation of the MS lesions severity.

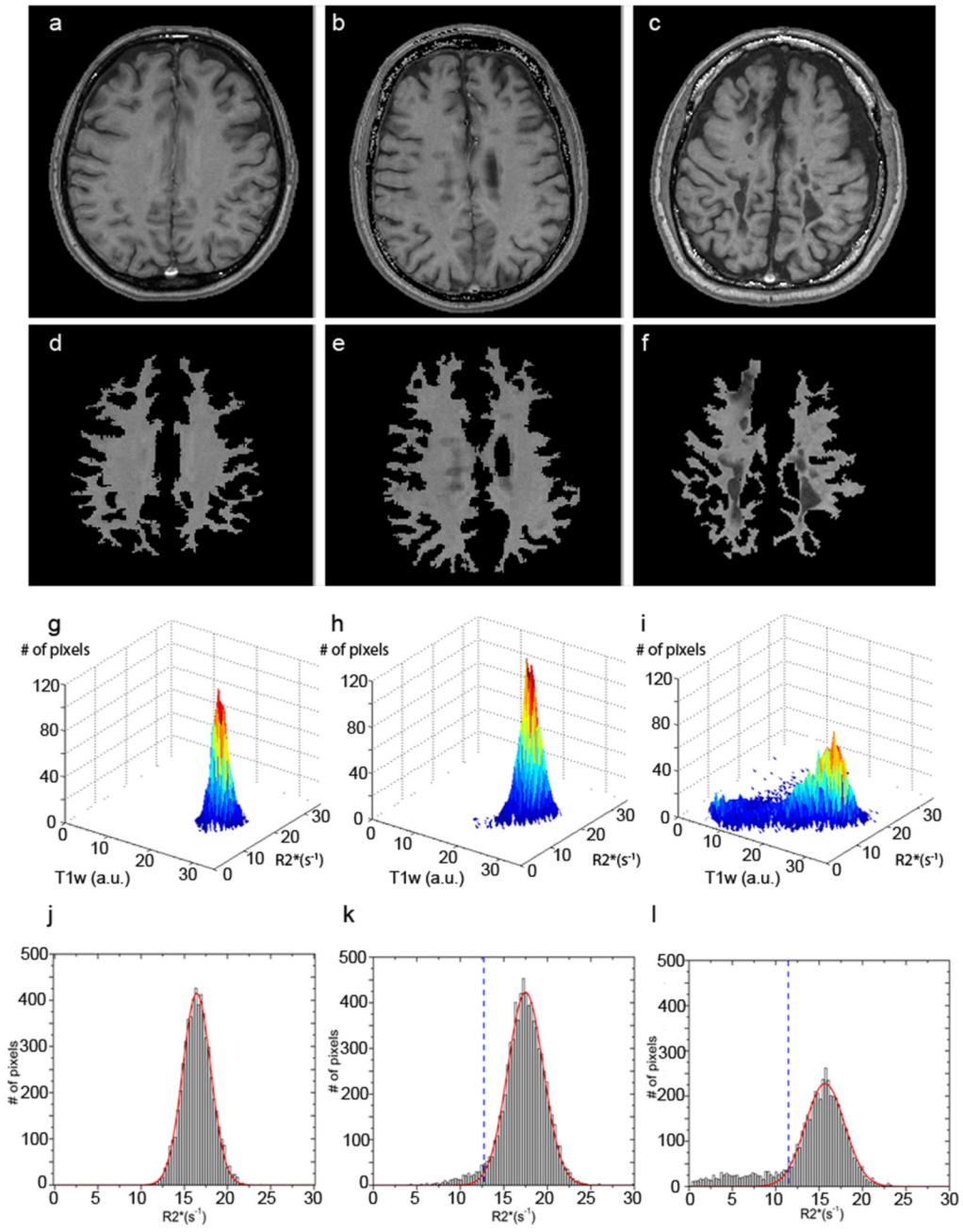

Figure 6.

Different steps of the proposed method for scoring MS severity: a), b) and c) are initial T1W-GEPCI images for three subjects represented in Figure 1 (healthy control), Figure 2 (MS #3), and Figure 3 (MS #5); d), e) and f) are the segmented T1W-GEPCI images using masks as described above; g), h), and i) are 3D histograms of the segmented voxels in the control subject, and subjects with RRMS and SPMS, respectively; j), k) and l) are the corresponding R2* histograms. Red lines represent Gaussian fits obtained by using only the upper half of the data in histograms and then extrapolated to all the other remaining R2* values. Note that histograms here are shown for selected images, not for the whole brain. Dashed blue lines represent threshold values defined for each slice. Notation a.u. stands for arbitrary unit.

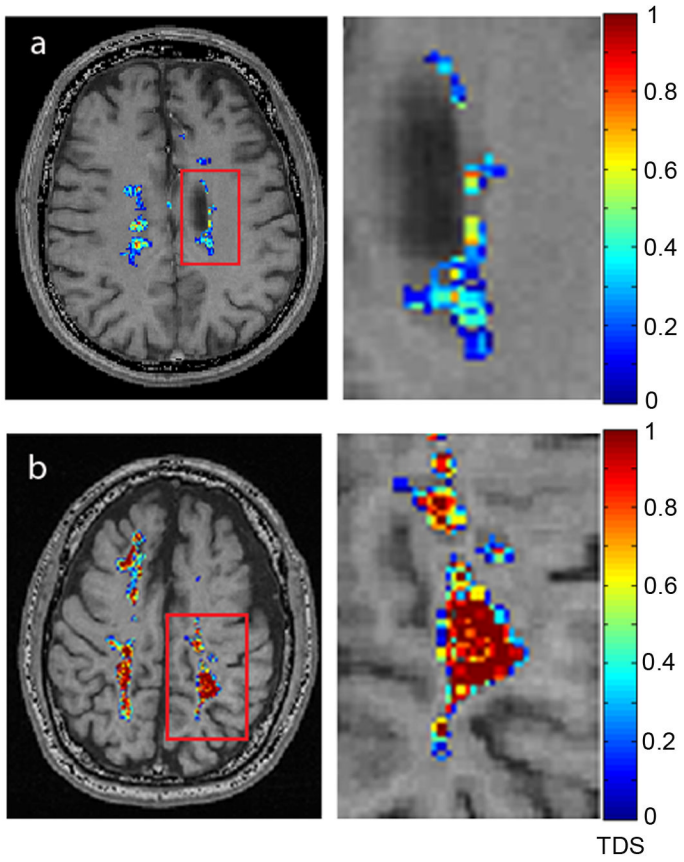

Figure 7.
Examples of images showing MS lesions with their tissue damage score (TDS) for a subject with RRMS (MS #3) and a subject with SPMS (MS #5). Magnified views on the right correspond to the areas highlighted by the red rectangles. The color bar represents severity score as defined by Eq [2]. The abnormal voxels (or lesions) were segmented according to the manual approach discussed above.

Table 1

Summary of the results for five control subjects (only mean and STD are provided) and five MS subjects. Quantitative results for tissue damage load (TDL), mean tissue damage score (MTDS) and lesion load (LL), are calculated using Eqs. [2] - [4]. Data of interest not only include characteristics determined by the "tail" of low R2* values located outside 1.96 peak width from peak center, but also the peak widths and center R2* relaxation rate constants. The nature of "abnormal" tissue in the control subjects is most likely due to variability of tissue structure, though errors in evaluating of tissue R2* values could also contribute to this effect. Note that practically all the scores in MS subjects are significantly different as compared to these "normal" values. p-values are determined with respect to corresponding distribution in normal subjects: (*) - $p<0.05$; (**) - $p<0.01$; (***) - $p<0.001$. Correlation coefficients for MTDS, peak width and peak center represent Pearson correlation coefficients. ($^{+}$) While TDL and LL also increase in concert with worsening disability on EDSS, the relationships are strongly non-linear, we, therefore, calculated Spearman rank correlation coefficients for the association between TDL and LL with EDSS.

Subject	TDL(mm^3)	LL(mm^3)	MTDS	peak width(s^{-1})	peak center(s^{-1})	EDSS
Control Mean	483	1913	0.251	3.39	16.74	-
Control STD	104	314	0.020	0.32	0.80	-
1 (RRMS)	797*	2706	0.295	3.61	15.88	2
2 (RRMS)	905*	3390*	0.267	3.33	16.99	3
3 (RRMS)	2698***	8022***	0.336*	4.00	17.60	4
4 (RRMS)	6479***	16509***	0.392**	3.93	15.00	6
5 (SPMS)	23204***	35853***	0.647***	5.10**	15.96	7
Correlation with EDSS	1.0^{+}	1.0^{+}	0.86	0.83	-0.41	